BEAM DYNAMICS INFLUENCE FROM QUADRUPOLE COMPONENTS IN FRIB QUARTER WAVE RESONATORS*

Z. He, Y. Zhang, Z. Zheng, Z. Liu, J. Wei, FRIB, Michigan State University, USA

Abstract

Non-axisymmetric RF cavities, such as quarter-wave resonators (QWRs), can produce axially asymmetric multipole field components that can influence beam dynamics. For example, dipole components can cause beam steering, an effect that has been well known to the community since 2001. However, higher order multipole field components, such as quadrupole components, which have potential influence on beam dynamics, have never received enough attention yet. In this paper, we choose FRIB QWRs as an example and quadrupole components are extracted by multipole expansion. Then, influence of quadrupole components on a single cavity is studied using thin lens model. After that, the influence of quadrupole components on a whole FRIB linac segment one is studied, and effects such as transverse profile ovalization and blow up of beam size are witnessed. Lastly, a possible way of quadrupole components compensation for FRIB driving linac is discussed.

INTRODUCTION

Non-axisymmetric RF cavities such as quarter-wave resonators (QWRs), half-wave resonators (HWR), spoke cavities and crab cavities, are now widely used in accelerators. Because of their geometry, dipole terms, quadrupole terms and other higher order multipole terms appear and can influence beam dynamics [1–4]. Dating back to 2001, A. Facco first pointed out possible beam steering effect coming from QWR and described the issue thoroughly in a later paper [1]. In the paper, a physics model is built to estimate the beam steering effect, and an easy way to compensate the steering effect using defocusing effect by shifting the beam axis is proposed.

Besides dipole term which causes beam steering, quadrupole term can cause beam shape deformation [2], and higher order terms can introduce non-linear effect and decrease dynamic aperture. By now, these effects haven't received enough attention yet. In this paper, we choose the QWR at FRIB [5] as an example. A scheme is developed to draw out multipole components through Fourier-Taylor multipole expansion. Then, a thin lens model based on transit time factor (TTF) [6, 7] is used to include multipole components into traditional cavity model. After that, the quadrupole effect is closely examined in both single cavity and whole linac segment one (LS1). At last, the possibility of self-cancelation of quadrupole components by fine tuning of solenoid polarity is discussed. The first two section has been discussed more thoroughly in our previous paper [8], here, we just list some important results in order to complete the whole story.

* The work is supported by the U.S. National Science Foundation under Grant No. PHY-11-02511, and the U.S. Department of Energy Office of Science under Cooperative Agreement DE-SC0000661

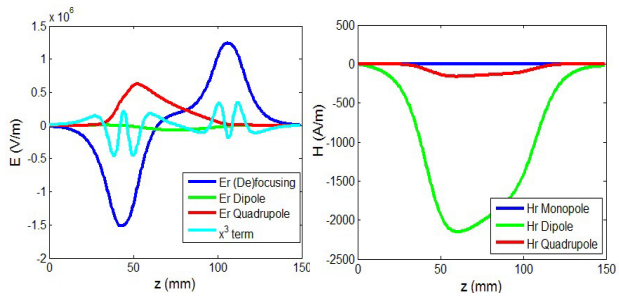

(a) (b)

Figure 1: Result of multipole strength curve for radial electric and magnetic field. (a) Radial electric field multipole strength. Blue curve is focusing term, green curve is dipole term, red curve is quadrupole term, and cyan curve is cubic term. (b) Radial magnetic field multipole strength. Blue curve is monopole term, green curve is dipole term, and red curve is quadrupole term.

FIELD MULTIPOLE EXPANSION

FRIB QWR 3D field simulated by CST [9] is chosen as the starting point and the numerical approach of Fourier-Taylor multipole expansion is used to draw out the field multipole terms. By expanding radial direction to Taylor series and azimuthal direction to Fourier series in a polar coordinate system, we are able to draw out multipole terms from a certain transverse E&M field to any arbitrary order. The process can be expressed as Eq. 1:

$$\begin{cases} F_{\rho,nm}(\rho,\theta) = F_{max}\sum_{n,m=0}^{\infty} P_n A_{nm} \Theta_m \\ P_n = \rho^n \\ \Theta_m = e^{im\theta} \end{cases} \quad (1)$$

By sampling all transverse plane along the longitudinal direction, we can get a plot indicating multipole strength along longitudinal direction, which is shown in Fig. 1.

MULTIPOLE THIN LENS MODEL

Assuming small thin lens kick, we can split the kick into electric part and magnetic part of contribution:

$$\Delta y' = \frac{qe\mu_0}{\gamma m_0}\int_{t_1}^{t_2} H_x(x,y,z,t)dt + \frac{qe}{\gamma m_0 \beta c}\int_{t_1}^{t_2} E_y(x,y,z,t)dt = \Delta y'_{H,y} + \Delta y'_{E,y} \quad (2)$$

ISBN 978-3-95450-173-1

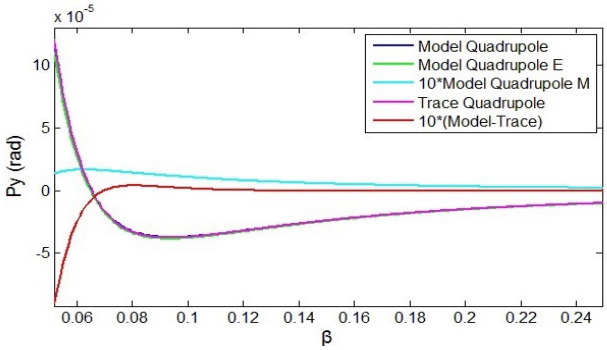

Figure 2: Prediction of quadrupole strength by model and tracking vs. β, synchronous phase $\phi_s = -\pi/6$ for β=0.085 QWR. Blue curve shows the total quadrupole strength calculated by model, green and cyan curve each stands for electric quadrupole and 10 times magnetic quadrupole by model, magenta curve shows result calculate from tracking, and red curve shows 10 times the error between model and tracking.

where q is the number of charge, e is the elementary charge amount, m_0 is the particle static mass, μ_0 is the permeability, c is the speed of light. Then, we absorb the time changing effect into the TTF factors and then we can easily derive the formulation for calculating the multipole thin lens kick:

$$\Delta y'_{E,y} = \frac{qe}{\gamma\beta^2 m_0 c^2} \sum_{i,j=0}^{n} t_{ij} V_{ij} (T_{ij} cos\phi - S_{ij} sin\phi)$$
$$\Delta y'_{H,y} = \frac{qe\mu_0}{\gamma\beta m_0 c^2} \sum_{i,j=0}^{n} t_{ij} U_{ij} (T_{ij} cos\phi - S_{ij} sin\phi) \quad (3)$$

$V_{ij}(U_{ij})$ is the strength of the multipole term i, j with a unit of Volt (Ampere). It is defined by integration of multipole term strength along longitudinal direction. T_{ij} and S_{ij} is the transit time factors of multipole term i, j. ϕ is the multipole phase. t_{ij} is the coordinate transferring factor, which is a constant for dipole term and is proportional to coordinate for focusing and quadrupole term.

From now, we put our focus mainly on quadrupole component. The term with $i = 1, j = 2$ stands for quadrupole term. For vertical electric field, $E_{max}(z) = E_{max,\rho}(z) = E_{max,\theta}(z)$, coordinate transferring factor $t_{ij} = y/\rho_{max}$; for magnetic field, $H_{max}(z) = H_{max,\rho}(z) = H_{max,\theta}(z), t_{ij} = y/\rho_{max}$. Calculation of FRIB $\beta = 0.085$ QWR quadrupole strength versus β can be seen in Fig. 2. Synchronous phase is fixed at $-\pi/6$. Good agreement between model and particle tracking result has been confirmed. According to the model, we can draw the conclusion that, quadrupole kick mainly comes from electric field and there is nearly no contribution from magnetic field. Quadrupole effect would be damping with β growing and would be more significant when at low β. The quadrupole polarity switched once at a certain β.

By putting the multipole thin lens kick at their electric center, it is easy to add multipole influence into traditional

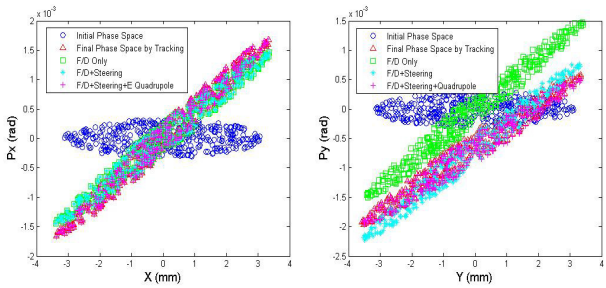

(a) (b)

Figure 3: X-Px phase space and Y-Py phase space of a KV distribution beam using tracking and model including different multipole terms of β=0.085 QWR, particle β is 0.055; (a), X-Px phase space; (b), Y-Py phase space.

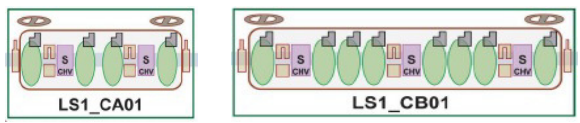

(a) (b)

Figure 4: Schematic plot of a single β=0.041 QWR cryomodule (a) and β=0.085 QWR cryomodule (b). Green oval represents RF cavity and magenta rectangle represents solenoid.

cavity model. Then, we track a whole cavity and compare the result with 3D field tracking. The result can be seen in Fig. 3. The $\beta = 0.085$ QWR is chosen, and a particular particle $\beta = 0.055$, where quadrupole component is quite large as indicated in Fig. 2, is used.

In Fig. 3, left figure is the X-Px phase space and right figure is the Y-Py phase space, particle β equals 0.055, synchronous phase is $-\pi/6$. Blue circle is the initial phase space. Red triangle is the result from 3D field tracking. Green square indicates phase space after adding defocusing term. After adding steering term, phase space become cyan star. After adding quadrupole term, phase space become magenta cross, which is close to 3D field tracking, with error down to 1% for momentum. As a result, we can see that, quadrupole term of QWR would influence beam dynamics significantly, and there is no way of modelling the beam to a high precision if the the quadrupole term is neglected.

QUADRUPOLE INFLUENCE ON LS1

FRIB LS1 is using two kinds of QWRs, mainly $\beta = 0.041$ QWR and $\beta = 0.085$ QWR. The lattice is following a cryomodule-based periodic structure, and each kind of QWR corresponds to a certain kind of cryomodule. The lattice for a single $\beta = 0.041$ or $\beta = 0.085$ cryomodule is shown in Fig. 4. There are 3 $\beta = 0.041$ cryomodules and 11 $\beta = 0.085$ cryomodules in LS1. An all-solenoid transverse focusing scheme is applied. The main advantage of all-solenoid focusing lattice is that it preserves round shape of a beam and provide convenience for beam matching.

ISBN 978-3-95450-173-1

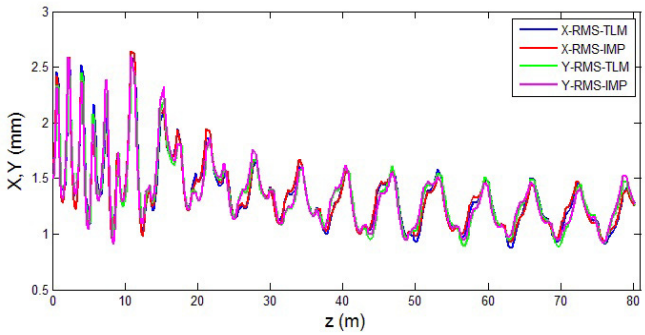

Figure 5: Benchmark thin lens model against IMPACT without the quadrupole term and for a round injection beam. Blue, X rms radius by thin lens model; Red, X rms radius by IMPACT; Green, Y rms radius by thin lens model; Magenta, Y rms radius by IMPACT.

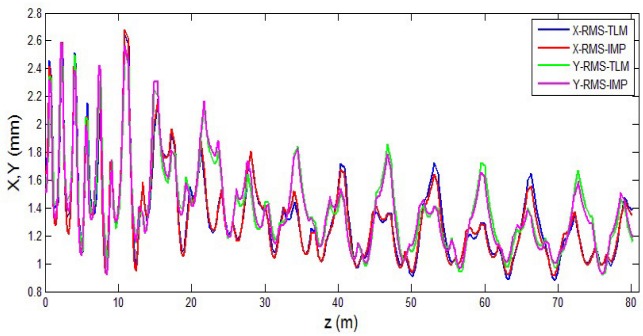

Figure 6: Benchmark thin lens model against IMPACT with the quadrupole term, and for a round injection beam, constant solenoid polarity. Blue, X rms radius by thin lens model; Red, X rms radius by IMPACT; Green, Y rms radius by thin lens model; Magenta, Y rms radius by IMPACT.

Then, we extend our simulation to the whole LS1. For the time being, we are using axisymmetric RF field. The model for solenoid is the traditional hard-edge model. The result is shown in Fig. 5. We can see that the model benchmarked very well with IMPACT [10], and round input beam persists to be round when no quadrupole term is considered.

Then, we can do the similar simulation by switching on the quadrupole component. For IMPACT case, the 3D field particle tracking scheme is used, and for the model, quadrupole thin lens kick is added. The result is shown in Fig. 6. As we can see, both IMPACT and model show discrepancy between x and y direction rms radius because of quadrupole effect, the initial round input beam become oval in shape. And the model is still good enough to benchmark with IMPACT with 3% of average error.

Transverse RMS plot alone isn't good enough to measure the ovalization effect quantitatively. Therefore, we define the L/S parameter, which equals the ratio between long axis and short axis for the oval shape transverse real space. We can calculate the L/S parameter from any theta matrix element by Eq. 4:

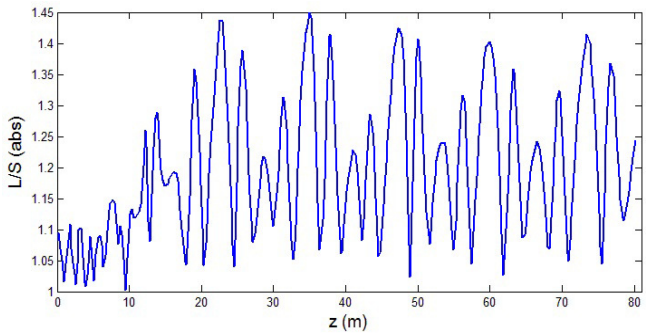

Figure 7: L/S line of constant solenoid polarity case.

$$L/S = \sqrt{\frac{\langle x^2\rangle + \langle y^2\rangle + \sqrt{(\langle x^2\rangle - \langle y^2\rangle)^2 + 4\langle xy\rangle^2}}{\langle x^2\rangle + \langle y^2\rangle - \sqrt{(\langle x^2\rangle - \langle y^2\rangle)^2 + 4\langle xy\rangle^2}}} \quad (4)$$

By using Eq. 4, we can calculate the L/S plot of Fig. 6, which can be seen in Fig. 7. The maximum value of L/S is around 1.45.

POSSIBILITIES OF SELF-CANCELATION OF QUADRUPOLE COMPONENTS

A straight forward way of taking care of the quadrupole component is to add correction quadrupoles at certain location. However, in this chapter, we are going to talk about a different way of self-cancelation of quadrupole components by fine tuning of solenoid polarity.

The original idea comes from comparison between original FRIB lattice design and updated FRIB lattice design. To avoid too strong coupling between horizontal and vertical direction, the original FRIB lattice is utilizing an alternative solenoid polarity scheme. However, after the insight of quadrupole components in QWR cavities, we find out that alternative solenoid polarity setting, which causes Larmor frameto rotate back-and-forth, thus having a clear anisotropic orientation, tends to add up quadrupole influence because quadrupole components mostly have the same polarity according to Fig. 2. The transverse rms size plot and L/S parameter plot for alternative solenoid polarity case can be seen in Fig. 8(a).

From Fig. 8(b), we can see that alternative solenoid polarity increases ovalization of the beam. L/S parameter climbs up to 1.9. That is why we decided to switch to constant solenoid polarity lattice. With Larmor frame constantly rotating towards the same direction, quadrupole components can possibly be smeared out due to self-cancellation. From Fig. 6 and Fig. 7, we can see that the scheme really works well.

However, constant polarity and alternative polarity are just two specific case of 2^{39} possible settings of all 39 solenoids in LS1. Constant polarity setting can provide perfect self-cancellation only when Larmor frame is rotating fast enough and when all quadrupole components have the same polarity

ISBN 978-3-95450-173-1

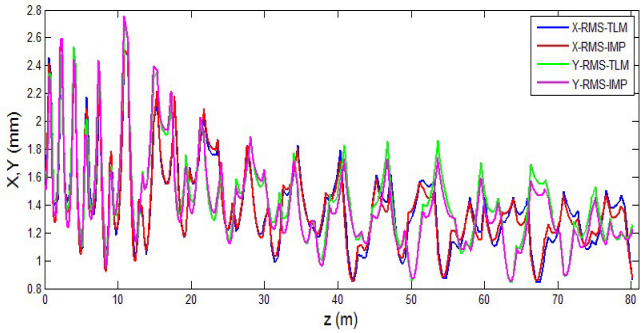

(a)

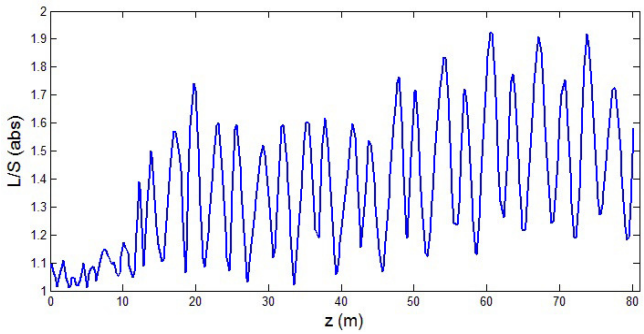

(b)

Figure 8: Transverse rms size plot and L/S parameter plot for a round injection beam, alternative solenoid polarity. (a) Benchmark of thin lens model against IMPACT, Blue, X rms radius by thin lens model; red, X rms radius by IMPACT; Green, Y rms radius by thin lens model; Magenta, Y rms radius by IMPACT. (b) L/S line of alternative solenoid polarity case.

and strength, which is quite far away from the real situation. So in theory, there could exist a better case where the solenoid polarity are fine tuned to better cancel out the quadrupole component. The schematic plot of the idea is shown in Fig. 9. If we come to a situation described by Fig. 9, we get two choice to rotate the beam according to the solenoid polarity, and rotating the beam counter clockwise would be better than clockwise. The real situation is not that simple and straight forward and a global optimization would be preferred.

Because we've got 39 solenoids and two possible polarity for each solenoid, we are solving a global optimization problem with 39 dimension and two possible value for each dimension. Thus, the Genetic Algorithm [11] is chosen as the global optimization algorithm. The characteristic volume (defined by mean value times standard deviation times maximum value) of L/S plot is chosen as the minimizing target. Thin lens model, which takes 50 ms per run is used instead of IMPACT, which uses particle tracking and is much slower, in the searching process. Fig. 10 shows one of the optimized cases.

From Fig. 10, we can see that, the quadrupole term largely got suppressed and transverse beam profile becomes closer to

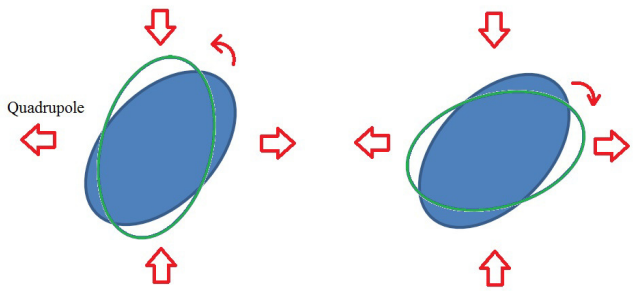

Figure 9: Schematic plot of possibility of self-cancelation of quadrupole component.

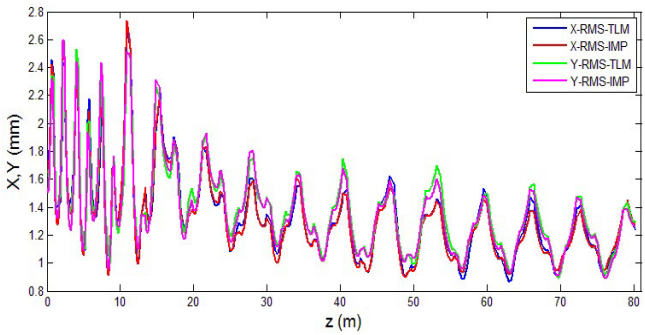

(a)

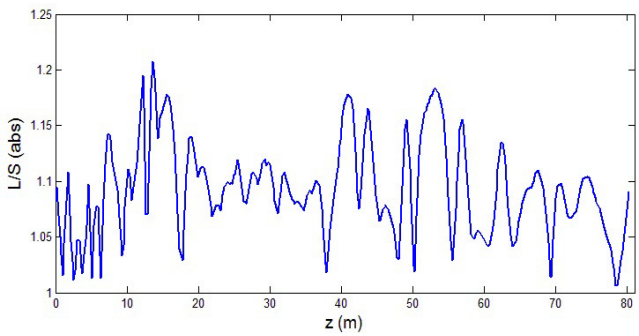

(b)

Figure 10: Transverse rms size plot and L/S parameter plot for a round injection beam, optimized solenoid polarity. (a) Benchmark of thin lens model against IMPACT, Blue, X rms radius by thin lens model; red, X rms radius by IMPACT; Green, Y rms radius by thin lens model; Magenta, Y rms radius by IMPACT. (b) L/S line of alternative solenoid polarity case.

ISBN 978-3-95450-173-1

circle, the maximum L/S parameter drops to around 1.2. The result confirms that it is possible to achieve self-cancelation of quadrupole components by fine tuning of solenoid polarity, and no extra component for correction is really needed.

However, we found out that, the global optimization method doesn't always give a fixed pattern, which implies that the optimum solenoid setting may not be stable and universal enough to be realistic and useful. Further study of the physics behind the scheme of self-cancelation of quadrupole components is needed before we can get something really useful.

CONCLUSION

Quadrupole components in non-axisymmetric RF cavities have been modelled by thin lens model which is based on multipole expansion of numerical 3D field. FRIB $\beta = 0.085$ QWR has been chosen as an example and we show the importance in taking quadrupole term into consideration when building the right linear model for the QWR. Study of the whole LS1 of FRIB indicates quadrupole term would significantly ovalize the originally round beam, and the amount of ovalization would highly depend on solenoid polarity. A comparison between constant solenoid polarity and alternative solenoid polarity shows that the constant solenoid polarity setting has less ovalization. A genetic algorithm is developed to further exploit the possibility of better self-cancelation of quadrupole component by fine tuning the solenoid polarity. An optimized solenoid polarity pattern shows better self-cancelation and the beam profile becomes closer to circle. More physics study is needed in order to come up with a universal and stable solenoid polarity pattern which can be useful.

ACKNOWLEDGMENT

The author would like to thank Prof. Chuanxiang Tang of Tsinghua University, on inspiring discussing on how to handle cavity multipole components. And J. Qiang, the author of the IMPACT code, on useful information about using IMPACT and understanding its physics behind. The author would also like to thank S. Lund, Q. Zhao, Y. Yamazaki and F. Marti for numerous helpful discussions. The work is supported by the U.S. National Science Foundation under Grant No. PHY-11-02511, and the U.S. Department of Energy Office of Science under Cooperative Agreement DE-SC0000661.

REFERENCES

[1] Alberto Facco and Vladimir Zvyagintsev. Beam steering in superconducting quarter-wave resonators: An analytical approach. *Physical Review Special Topics-Accelerators and Beams*, 14(7):070101, 2011.

[2] Marco Cavenago. Determining the radiofrequency dipole and quadrupole effects in quarter wave resonators. *Nuclear Instruments and Methods in Physics Research Section A: Accelerators, Spectrometers, Detectors and Associated Equipment*, 311(1):19–29, 1992.

[3] RG Olave, JR Delayen, and CS Hopper. Multipole expansion of the fields in superconducting high-velocity spoke cavities. *Proc. LINAC2012, Tel-Aviv Israel, MOPB072*, 2012.

[4] SU De Silva and Jean R Delayen. Design evolution and properties of superconducting parallel-bar rf-dipole deflecting and crabbing cavities. *Physical Review Special Topics-Accelerators and Beams*, 16(1):012004, 2013.

[5] J Wei, D Arenius, E Bernard, N Bultman, F Casagrande, S Chouhan, C Compton, K Davidson, A Facco, V Ganni, et al. The frib project–accelerator challenges and progress. *HIATC2012, Chicago, USA*, 51, 2012.

[6] Thomas P Wangler. *RF Linear accelerators*. John Wiley & Sons, 2008.

[7] Kenneth R Crandall. Trace 3-d documentation. Technical report, Los Alamos National Lab., NM (USA), 1987.

[8] Zhengqi He, Zhihong Zheng, Zhengzheng Liu, Yan Zhang, and Jie Wei. An analytical cavity model for fast linac-beam tuning. In *Proc. of LINAC*, volume 12, 2012.

[9] CST Microwave Studio. Computer simulation technology. *GmbH, Darmstadt, Germany*, 2009.

[10] Ji Qiang, Robert D Ryne, Salman Habib, and Viktor Decyk. An object-oriented parallel particle-in-cell code for beam dynamics simulation in linear accelerators. In *Proceedings of the 1999 ACM/IEEE conference on Supercomputing*, page 55. ACM, 1999.

[11] David E Goldberg. *Genetic algorithms*. Pearson Education India, 2006.

ISBN 978-3-95450-173-1